ACS APPLIED MATERIALS & INTERFACES

Research Article

www.acsami.org

Smart IR780 Theranostic Nanocarrier for Tumor-Specific Therapy: Hyperthermia-Mediated Bubble-Generating and Folate-Targeted Liposomes

Fang Guo, Meng Yu, Jinping Wang, Fengping Tan,* and Nan Li*

Tianjin Key Laboratory of Drug Delivery & High-Efficiency, School of Pharmaceutical Science and Technology, Tianjin University, 300072 Tianjin, People's Republic of China

ABSTRACT: The therapeutic effectiveness of chemotherapy was hampered by dose-limiting toxicity and was optimal only when tumor cells were subjected to a maximum drug exposure. The purpose of this work was to design a dual-functional thermosensitive bubble-generating liposome (BTSL) combined with conjugated targeted ligand (folate, FA) and photothermal agent (IR780), to realize enhanced therapeutic and diagnostic functions. This drug carrier was proposed to target tumor cells owing to FA-specific binding, followed by triggering drug release due to the decomposition of encapsulated ammonium bicarbonate (NH_4HCO_3) (generated CO_2 bubbles) by being subjected to near-infrared (near-IR) laser irradiation, creating permeable defects in the lipid bilayer that rapidly release drug. *In vitro* temperature-triggered release study indicated the BTSL system was sensitive to heat triggering, resulting in rapid drug release under hyperthermia. For *in vitro* cellular uptake experiments, different results were observed on human epidermoid carcinoma cells (KB cells) and human lung cancer cells (A549 cells) due to their different (positive or negative) response to FA receptor. Furthermore, *in vivo* biodistribution analysis and antitumor study indicated IR780-BTSL-FA could specifically target KB tumor cells, exhibiting longer circulation time than free drug. In the pharmacodynamics experiments, IR780-BTSL-FA efficiently inhibited tumor growth in nude mice with no evident side effect to normal tissues and organs. Results of this study demonstrated that the constructed smart theranostic nanocarrier IR780-BTSL-FA might contribute to establishment of tumor-selective and effective chemotherapy.

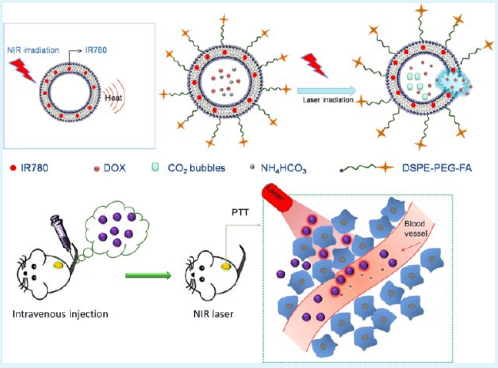

KEYWORDS: *IR780, hyperthermia-mediated, bubble thermosensitive liposomes, folate-receptor targeted, doxorubicin, tumor chemotherapy*

1. INTRODUCTION

Currently, chemotherapy is still the treatment of choice for many types of tumors. However, the major obstacle in current antitumor chemotherapy has been low tumor selectivity due to the nontargeted delivery of the drug, producing considerable adverse effects. A wide range of biocompatible, nontoxic nanocarriers such as liposomes, polymeric micelles, and nanoparticles have been developed to selectively accumulate in the tumor compartment via a passive targeting mechanism termed the enhanced permeability and retention (EPR) effect.[1] Nevertheless, these delivery systems have displayed several intrinsic limitations due to the lack of specificity. Great efforts have been made to overcome the limitations. For example, tumor microenvironment sensitive nanocarriers that responded to changes in environmental conditions, such as temperature, pH value, electromagnetic fields, and light, have received great attention for their advantages in application for targeted drug delivery.[2−4]

Various types of nanocarriers with stimuli-sensitive properties have been studied to increase local concentration of therapeutic molecules at the target tissues. A typical example was thermosensitive liposomes (TSL), which could immediately release encapsulated drugs in response to mild hyperthermia in tumor sites. TSL showed three main advantages compared with the conventional long-circulating PEGylated liposomes. First, TSL released the drug at hyperthermic temperature (40−42 °C) in such a rapid way which could resist fast blood passage time and wash out of the encapsulated drug from the tumor. Second, the TSL drug delivery system remained stable at 37 °C; thereby it could keep the drug within the liposomes during blood transport. Finally, TSL in combination with mild hyperthermia could selectively increase the local drug concentration and lead to an evident improvement in therapeutic efficacy.

In recent study, a cationic liposomal carrier that contained ammonium bicarbonate (NH_4HCO_3) was developed.[5] The NH_4HCO_3-containing thermosensitive liposome was denoted as bubble-generating thermosensitive liposomes (BTSL). The key component NH_4HCO_3 could be readily incorporated into an aqueous compartment of liposomes. Upon heating to a high temperature (40−42 °C), it could quickly decompose to generate CO_2 bubbles. As a result, on one hand, after the internalized liposomes went through endocytosis and intracellular trafficking

Received: April 23, 2015
Accepted: August 31, 2015
Published: August 31, 2015

DOI: 10.1021/acsami.5b06552
ACS Appl. Mater. Interfaces 2015, 7, 20556−20567

Scheme 1. Illustration of the Constructed Theranostic Liposomes (a) Illustrating the Photothermal Therapy of IR780 Liposomes Following Near-IR Light Irradiation (Showing the Structure of IR780-BTSL-FA and the Mechanism of Localized Drug Release As Triggered by Heat); (b) Specific Targeting Effect of IR780-BTSL-FA and Cellular Uptake Procedure

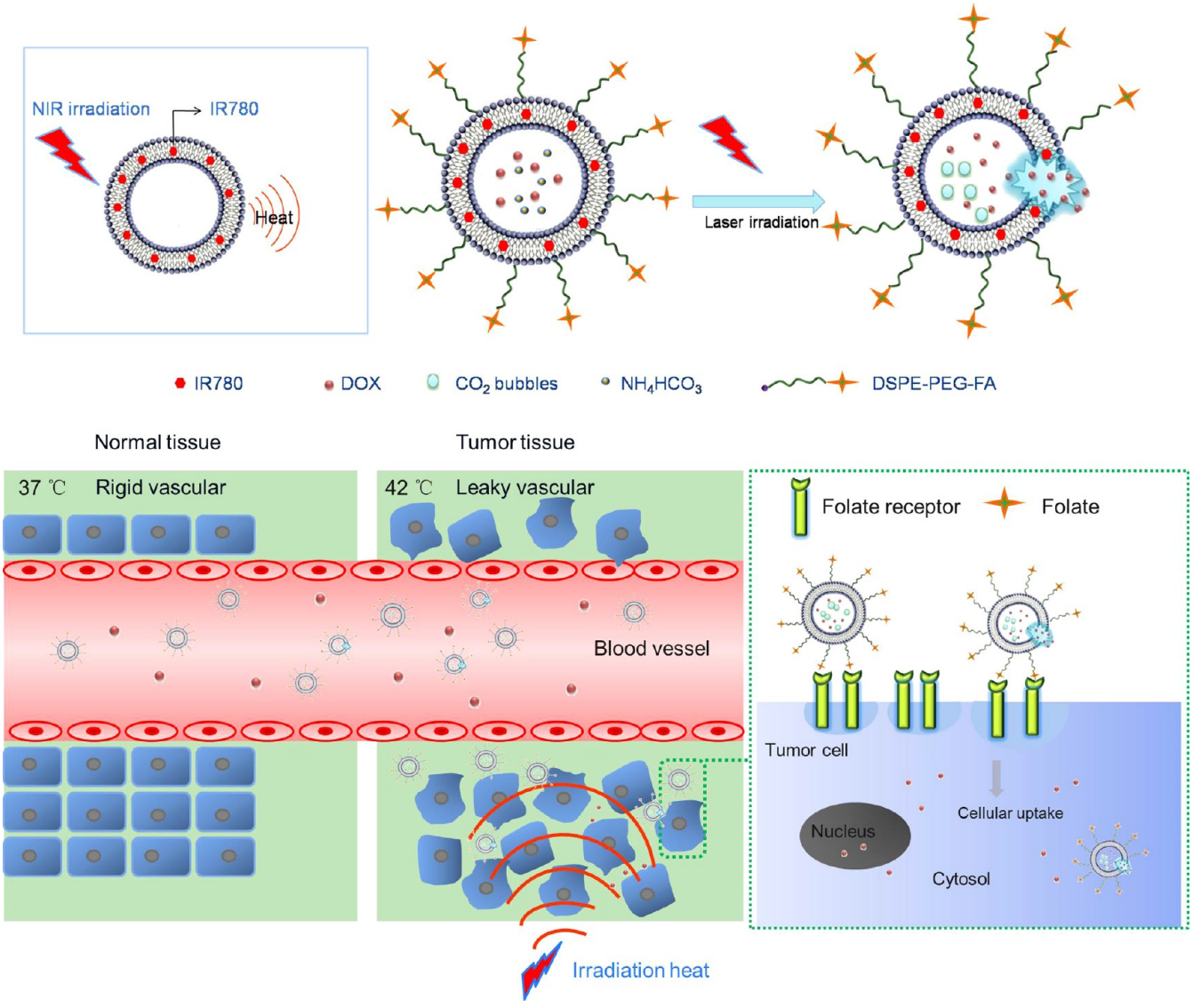

to lysosomes, they could be hyperthermia-triggered to generate CO_2 bubbles, which were formed and grew transiently followed by collapse of the bubbles. Accordingly, the lysosomal membranes were disrupted to release proteases into the cytosol, leading to cell necrosis. On the other hand, after CO_2 bubbles generation and collapse, the produced disruptive force subsequently created permeable defects in the lipid bilayer and ultimately induced a rapid drug release to instantly increase the drug concentration locally.

Although BTSL could improve the targeting drug delivery to some extent by physical heating, there were still some problems to solve, such as actively transporting drug to specific tumor sites after intravenous injection, the triggered release method, and so on. For the first problem, the introduction of various biological ligands or antibodies into drug delivery systems provided the opportunity for selectivity drug delivery to the tumor cell.[6−8] Folate (FA) was a small molecular ligand which has high affinity (K_d ~ 0.1−1 nmol/L) for the folate receptor (FR).[9−12] Studies have shown FA-targeted drug delivery could bypass the efflux pump of P-glycoprotein (P-gp), thereby improving the drug accumulation in a tumor to increase multidrug resistance (MDR) reversing effect.[13,14] In this study, FA would be used to modify the surface of BTSL to elevate its targeting ability to tumor cells. For the second problem, in recent years, significant attention has been paid to develop near-IR dyes as a photothermal agent in tumor treatment.[15−19] IR-780, a representative stable hydrophobic near-IR fluorescence dye, was capable of fluorescent imaging and photothermal heating which combined diagnostic and photothemal therapies together.[18]

On the basis of the above background, in this work, we hypothesized to construct a smart-triggered drug delivery system (IR780-BTSL-FA) which integrated targeting, therapeutic, and diagnostic functions together, providing many potential advantages (a schematic of the new system was shown in Scheme 1): (1) The BTSL would be used as a smart carrier, which was stable in the blood circulation and was triggered via heat stimulus in the tumor site; (2) IR780-mediated photothermal heating could trigger the drug release from the temperature-sensitive membrane of BTSL as well as *in vitro* and *in vivo* imaging; (3) FA ligand would be conjugated with the surface of the BTSL as

DOI: 10.1021/acsami.5b06552
ACS Appl. Mater. Interfaces 2015, 7, 20556−20567

Table 1. Composition of Different DOX-Loaded Liposome Formulations[a]

formulation	DPPC (mol)	Chol (mol)	DSPE-PEG$_{2000}$ (mol)	DSPE-PEG$_{2000}$-FA (mol)	IR780 (mol)
IR780-TSL	65	30	5		2
IR780-BTSL	65	30	5		2
IR780-BTSL-FA	65	30	4	1	2

[a]FA, folate; TSL, thermosensitive liposomes ($(NH_4)_2SO_4$); BTSL, bubble thermosensitive liposomes (NH_4HCO_3); BTSL-FA, FA-modified BTSL, respectively.

the active targeting moiety positioning to the specific tumor cells. The most commonly used antitumor agent doxorubicin (DOX) was treated as a model drug in this work. Accordingly, the objective of this work was to study the targeting accumulation effect and to evaluate the antitumor efficiency of the new carrier both *in vitro* and *in vivo*.

2. MATERIALS AND METHODS

2.1. Materials. DOX (99%) was obtained from Beijing Huafeng United Technology Co., Ltd. (Beijing, China). The heptamethine indocyanine dye IR-780 iodide was obtained from Sigma-Aldrich Co. LLC (St. Louis, MO, USA). Dipalmitoylphosphatidylcholine (DPPC), 1,2-distearyl-*sn*-glycero-3-phosphoethanaolamine-*N*-[methoxypoly-(ethylene glycol)-2000] (DSPE-PEG$_{2000}$), DSPE-PEG$_{2000}$-FA, and cholesterol (Chol) were purchased from Avanti Polar Lipids (Alabaster, AL, USA). Fetal bovine serum (FBS) and FA were provided by HEOWNS Biochemical Technology Co., Ltd. (Tianjin, China). The nuclei dye 4′,6-diamidino-2-phenylindole (DAPI) was obtained from Tianjin Real Sungene Biotechnology Co., Ltd. (Tianjin, China). Other chemicals and reagents were of analytical grade.

2.2. Preparation of Liposomes. Liposomes colloidal suspensions were prepared by using thin-film hydration method, followed by membrane extrusion.[20,21] IR780 and lipid mixtures (see Table 1) were dissolved in a mixed solvent of chloroform and methanol. Then the organic solvent was removed with rotavapor to generate a thin lipid film on the glass vial. The lipid film was then hydrated with an aqueous $(NH_4)_2SO_4$ (300 mM) or NH_4HCO_3 (3 M) solution via sonication at room temperature and followed by sequential extrusions through 800, 400, 200, and 100 nm polycarbonate filters (five times each). The free $(NH_4)_2SO_4$ and NH_4HCO_3 were removed by dialysis method (10 wt % sucrose solution with 5 mM NaCl). DOX (drug:lipid = 1:10, w/w) was subsequently mixed with the suspension and incubated at room temperature for 24 h. Finally, the unencapsulated DOX was removed by passing through a Sephadex G-50 column (GE Healthcare, Chalfont St Giles, U.K.). After separation, the amount of DOX entrapped within the liposomes was determined by fluorescence spectrometer method. The entrapment efficiency (EE%) of liposomes was expressed according to the following equation:

$$EE/\% = (W_{encapsulated}/W_{total}) \times 100$$

where $W_{encapsulated}$ was the amount of entrapped DOX and W_{total} represented the total amount of DOX.

2.3. Characterization of Test Liposomes. The mean diameter, particle size distribution, and ζ potential were measured by Malvern Zetasizer Nano (Malvern Instruments Ltd., Malvern, U.K.). Particle morphology was detected by a JEM-100CXII transmission electron microscope (TEM, JEOL, Tokyo, Japan) followed by negative staining procedure using phosphotungstic acid. Atomic force microscopy (AFM, Nanowizarc, JPK Ltd., Berlin, Germany) was used to further observe the surface morphology of BTSL and BTSL-FA. The liposomal formulation was diluted with distilled water and was then spread on a mica sheet, dried at room temperature.

The temperature profile of IR780-BTSL-FA during near-IR laser irradiation (780 nm, 1 W/cm^2) was obtained with a thermocouple needle.

2.4. *In Vitro* Temperature Triggered Release of Liposomes. DOX released from IR780-TSL, IR780-BTSL, and IR780-BTSL-FA (at 37 and 42 °C) was performed using a dialysis technique. DOX release behavior from IR780-BTSL-FA with and without laser irradiation for 5 min at initial time of the experiment was also investigated (780 nm, 1 W/cm^2). Generally, an aliquot of each DOX-loaded liposome (0.5 mL) was placed into a dialysis tube (MW = 8−14 kDa) and immersed in 30 mL of PBS (pH 7.4) containing 10% FBS, followed by magnetic stirring at 50 rpm. At predetermined time points, 0.5 mL of release medium was sampled and replaced with an equal volume of fresh release medium. The amount of DOX released was determined by fluorescence intensity using a fluorescence spectrometer (Ex = 485 nm, Em = 570 nm) at each time intervals.

2.5. Cell Cultures. In this work, KB cells and A549 cells were used to evaluate the targeting effect of the constructed nanocarrier, as the two cell lines were reported to be of FR overexpression (positive cell model) and lack FR expression (negative cell model), respectively. The DMEM, RPMI 1640 solution, and medium supplement with 10% FBS, 100 IU/mL penicillin, and 100 μg/mL streptomycin were utilized as the cell culture medium. Cells were cultivated at 37 °C in a 5% CO_2 atmosphere.

2.6. *In Vitro* Cellular Uptake. To observe the cellular delivery of DOX-loaded liposomes with or without FA-targeting delivery system, KB and A549 cells were seeded at a density of 1×10^5 in 6-well plates, respectively. After 24 h incubation at 37 °C, the culture medium was replaced by fresh medium containing the PBS (control), free DOX, IR780-TSL, IR780-BTSL, and IR780-BTSL-FA (after the liposomal formulations were added, the medium was heated to 42 °C for 30 min) at the same dosage of DOX. For competitive binding studies, 20 μL of free FA (1 mM) was added to each well 2 h before the addition of liposomes. After 4 h, the cells were rinsed twice with PBS and then detached with trypsin. Finally, the cells were resuspended in PBS and subjected to a FACScan flow cytometry (BD FACSCalibur).

The fluorescent images of cells were analyzed using a laser scanning confocal microscope (Olympus, Tokyo, Japan). The cells were washed three times with PBS (pH 7.4) and then fixed in 4% formaldehyde in PBS (pH 7.4), followed by nucleus staining with DAPI (blue) for 20 min at room temperature. The fluorescence signal was imaged at λ_{Ex} (485 nm) for DOX and at λ_{Ex} (633 nm) for IR780.

2.7. *In Vitro* Cytotoxicity. Cytotoxicity of each formulation was evaluated by MTT assay with KB cells and A549 cells. The cells were seeded into a 96-well plate for 24 h (5×10^3 cells/well) and then incubated at 37 °C with 5% CO_2. The supernatants were discarded, and the cells were washed twice with PBS (pH 7.4). Free DOX, DOX-loaded liposome (IR780-TSL, IR780-BTSL, and IR780-BTSL-FA), or blank IR780-BTSL-FA was put into the culture medium for 4 h at a DOX concentration of 10, 20, 40, 80, or 100 μg/mL, respectively. The culture medium without DOX (PBS) was put in the wells for control groups. Then 20 μL of MTT solution (5.0 mg/mL) was added to each well, and the cells were further incubated for 4 h at 37 °C. Next, the medium was removed, and then 200 μL of dimethyl sulfoxide (DMSO) was put in the well to dissolve the formazan crystals formed by the living cells. The absorption was recorded at 570 nm using a microplate reader (Thermo Scientific Varioskan Flash, Waltham, MA, USA). The *in vitro* efficacy and *in vitro* toxicity of free DOX and DOX-loaded or blank liposomes were expressed as cell viability, defined by the following equation:

$$\text{cell viability}/\% = [(I_0 - I_1)/I_0] \times 100$$

where I_0 was the absorbance of the cells incubated with the culture medium and I_1 was the absorbance of the cells incubated with different formulations (the presence or absence of near-IR irradiation of 780 nm, 1 W/cm^2 laser irradiation for 15 min).

2.8. Animals and Tumor Model. Female BALB/c nude mice (20 ± 2 g, 4−6 weeks old) were purchased from the Institute of Radiation

DOI: 10.1021/acsami.5b06552
ACS Appl. Mater. Interfaces 2015, 7, 20556−20567

Table 2. Entrapment Efficiency (EE), Drug Loading (DL), Mean Particle Size, and Polydispersity Index (PDI) of DOX Liposome Formulations[a]

formulation	EE (%)	DL (%)	size (nm)	PDI
IR780-TSL	77.8 ± 3.9	2.13 ± 0.09	104 ± 16	0.162 ± 0.009
IR780-BTSL	75.9 ± 6.0	2.07 ± 0.12	135 ± 9	0.342 ± 0.011
IR780-BTSL-FA	82.2 ± 4.8	2.25 ± 0.16	127 ± 3	0.264 ± 0.013

[a]Mean ± standard deviation; $n = 3$.

Medicine, Chinese Academy of Medical Sciences (Tianjin, China). The mice were raised to establish solid tumor models. KB cells (1×10^7) were administered by subcutaneous injection into the flank region of the mice. Tumor volume was calculated as (tumor length) × (tumor width)^2/2.

When the tumors reached about 200 mm^3, the mice were randomly divided into eight groups ($n = 6$) and received intravenous administration of saline, free DOX, IR780-TSL (with and without laser), IR780-BTSL (with and without laser), and IR780-BTSL-FA (with and without laser) at 10 mg of DOX/(kg of body weight) via tail vein, respectively. For the groups with laser irradiation, the mouse's left leg was subjected to 780 nm, 1 W/cm^2 near-IR laser irradiation for 15 min. The tumor volume and body weight were calculated every day after the first injection.

2.9. *In Vivo* Imaging and Biodistribution Analysis. The *in vivo* imaging and distribution of the liposomes was analyzed by a noninvasive *in vivo* optical imaging technique.[22] The tumor model was developed as described in section 2.8. The mice were treated with free DOX, IR780-TSL, IR780-BTSL, and IR780-BTSL-FA (10 mg of DOX/(kg of body weight)) by iv injection, respectively. Each mouse's left leg was subjected to 780 nm, 1 W/cm^2 near-IR laser irradiation for 15 min. At 2 and 12 h postinjection, the *in vivo* near-IR fluorescence imaging was performed with a Kodak IVIS Spectrum system (500−750 nm emission fluorescence). The excitation and emission wavelength of IR780 was 704 and 730−750 nm, respectively. At 12 h postinjection, the mice were sacrificed and the organs including heart, liver, spleen, lung, and kidneys were also collected for imaging and *in vivo* biodistribution analysis. The excised tumors and organs were fixed in formalin, embedded in paraffin, sectioned into slices, and further stained with hematoxylin and eosin (H&E) to observe organ defects.

2.10. Statistical Analysis. The data from each treatment group and control are presented as mean ± SD. Student's t test and one-way analyses of variance (ANOVA) were performed in statistical analysis. The differences were considered significant when $p < 0.05$, and highly significantly when $p < 0.01$.

3. RESULTS AND DISCUSSION

3.1. Preparation and Characterization of Liposomes. Three types of liposomes including IR780-TSL, IR780-BTSL, and IR780-BTSL-FA were fabricated via film evaporation method, followed by sequential extrusion. A loading technique was applied to actively load DOX into test liposomes based on transmembrane NH_4HCO_3 (or $(NH_4)_2SO_4$) gradient. Table 1 listed the composition of each liposomal formulation. Table 2 summarized the important characteristics of the liposomes, including mean diameter, EE, and PDI value. All of the liposomes showed good homogeneity, with PDIs below 0.350 and average particle sizes between 104 and 135 nm. The constructed PEGylated liposomes with the appropriate particle size facilitated the vesicles to be transported in the vasculature of the tumor tissue and accumulated in the tumor site by the EPR effect.[1,23,24]

Furthermore, an efficient loading of DOX into the aqueous phase of each formulation (EE > 75%) was attained. The TEM study showed the regular circular shape of the liposomes (Figure 1) without any differences between IR780-BTSL and IR780-BTSL-FA. AFM was further used to confirm the particle surface morphology of the liposomes modified with FA ligand (as shown in Figure 1d−g). The results suggested the surface of nontargeted liposomes (IR780-BTSL) was relatively smooth, while the FA-targeted liposomes had small globular protrusions, which really verified the successful modification of liposomes with FA ligand.[25]

To evaluate the photothermal effect of IR780-BTSL-FA, we determined the temperature changes under laser irradiation *in vitro*. The maximum temperature of free IR780 or IR780-BTSL-FA increased to 54.9 or 68.2 °C with the laser irradiation at 780 nm (1 W/cm^2 for 300 s), while PBS as a negative control did not trigger significant temperature increase (Figure 2a). As a result, the quickly increased temperature (over 42 °C) of IR780-BTSL-FA under near-IR irradiation could lead to irreversible cell damage.[26−34]

3.2. *In Vitro* Temperature-Triggered Release. Figure 2c illustrated the *in vitro* DOX release profiles from the test liposomes at 37 °C (physiological temperature) and 42 °C (hyperthermic temperature), respectively. The data implied drug release from various liposomes exhibited temperature-dependent characteristic (release was considerably lower at 37 °C, but higher at 42 °C). Furthermore, drug release from the IR780-BTSL system was approximately 90% at 42 °C, which was significantly higher than that from IR780-TSL (53%).

When the local temperature was heated to 42 °C, IR780-BTSL exhibited considerable fast drug release within 10 min (>60%) (Figure 2c). Nevertheless, less than 10% DOX was released from IR780-TSL in 10 min at 42 °C, in spite of significant amounts of DOX (above 50%) being released in 24 h. In addition, although there was minor drug leakage (less than 25%) at physiological temperature (37 °C), the BTSL system still retained a large amount of DOX within the liposomes. These experimental results suggested that DOX encapsulation for the BTSL system was relatively stable at 37 °C, leading to the drug being maintained within the liposomes during blood circulation. However, the drug release would be faster when the carrier was under triggered temperature, which might create a high drug concentration gradient to facilitate diffusion of the drug into the tumor tissue. The fast-triggered drug release also acquired the ability to prevent rapid passage of the bloodstream and being washed out from the tumors.[35] Noteworthy, the property of sensitivity to heat triggering of the BTSL system was attributed to NH_4HCO_3 encapsulated in the liposomes. When liposomes were subjected to local heating over 42 °C, the decomposition of the encapsulated NH_4HCO_3 facilitated immediate thermal activation of CO_2 bubbles generation (transient formation, growth, and collapse of CO_2 bubbles), resulting in a disruptive force similar to the cavitation effect.[5]

Furthermore, the effect of laser irradiation on drug release behavior was also investigated (Figure 2b). IR780-BTSL-FA exhibited drug release of 29.5% by 8 h and the total release of 41.8% by 36 h without laser irradiation. In contrast, after laser irradiation, IR780-BTSL-FA released 75.4% DOX by 8 h and the total drug release amount was significantly increased to 91.1% by

DOI: 10.1021/acsami.5b06552
ACS Appl. Mater. Interfaces 2015, 7, 20556−20567

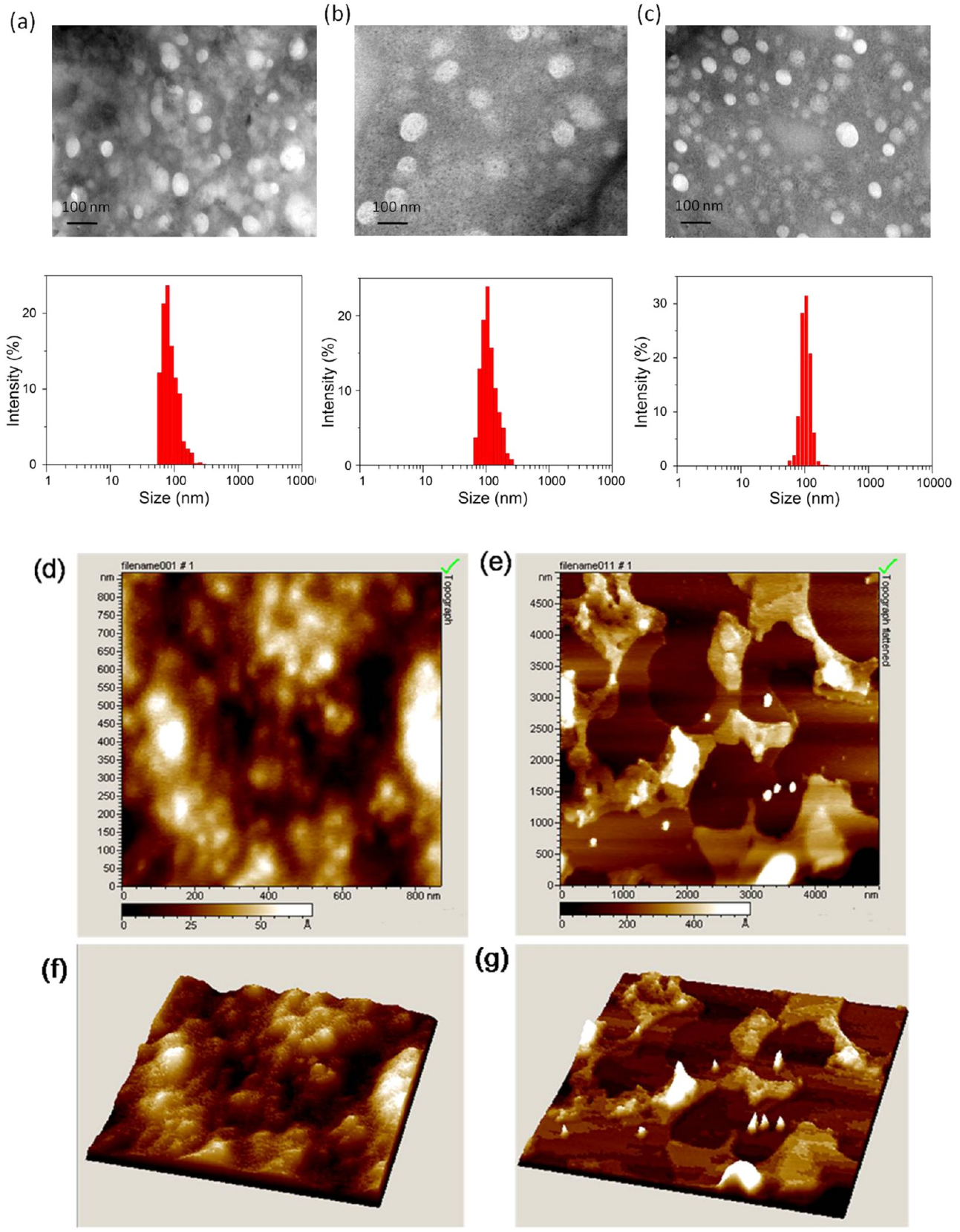

Figure 1. TEM images and particle distributions for (a) IR780-TSL, (b) IR780-BTSL, and (c) IR780-BTSL-FA. AFM spectra for (d, f) IR780-BTSL and (e, g) IR780-BTSL-FA ((d, e) plane surface image; (f, g) three-dimensional images).

36 h, indicating that the laser irradiation could effectively accelerate DOX release from IR780-BTSL-FA. The reason was because IR780-BTSL-FA increased in temperature over 42 °C under irradiation excitation so that triggered rapid drug release (Figure 2a). This effect was consistent with the results of liposomes subjected to local heating (Figure 2c).

DOI: 10.1021/acsami.5b06552
ACS Appl. Mater. Interfaces 2015, 7, 20556−20567

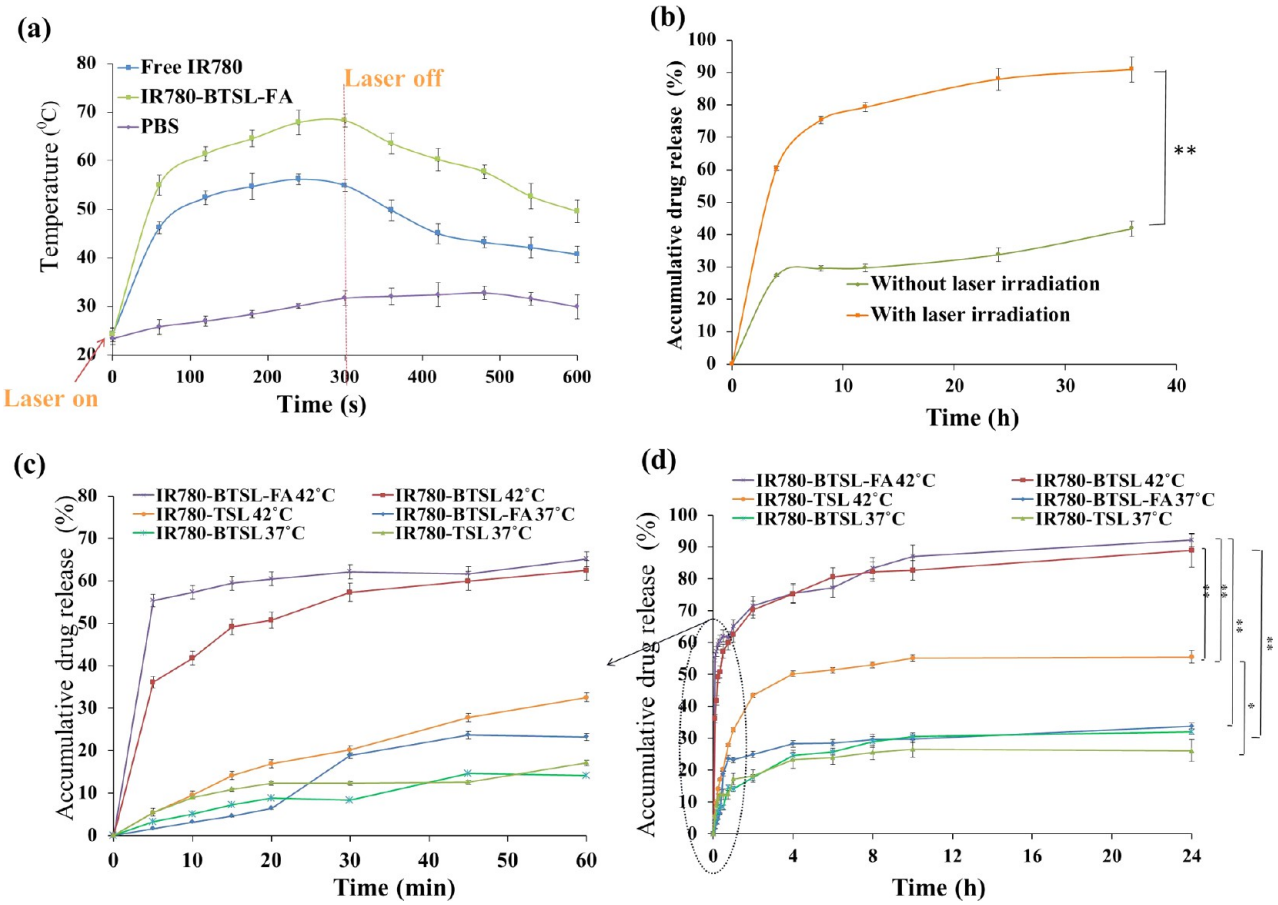

Figure 2. (a) Photothermal effect of PBS, free IR780, and IR780-BTSL-FA under continuous 780 nm laser irradiation (lasted for 5 min and then shut off). (b) DOX release profiles from IR780-BTSL-FA with and without laser irradiation. The data are shown as mean ± SD (n = 3); (*) $p < 0.05$, (**) $p < 0.01$. (c and d) *In vitro* temperature-triggered release profiles of DOX from liposomes incubated at 37 and 42 °C (n = 6) release profiles.

3.3. *In Vitro* Targeted Delivery Study. *3.3.1. In Vitro Cellular Uptake and Competitive Binding Assay.* FA was able to be efficiently internalized into the cells through the receptor-mediated endocytosis even when conjugated with a wide variety of molecules.[32,36] In this study, the targeting effect of IR780-BTSL-FA was evaluated by confocal laser scanning microscopy (CLSM). As shown in Figure 3a, free DOX was primarily localized to cell nuclei in KB cells and A549 cells after 4 h incubation, which was consistent with a previous report.[37] The significantly stronger red fluorescence in nuclei of IR780-BTSL-treated KB cells (compared to those of IR780-TSL) indicated the improvement of intracellular uptake of DOX. Notably, IR780-BTSL-FA formulation showed the highest intracellular uptake in KB cells (with strongest red fluorescence distribution), which was approximately to free DOX, while, for A549 cells, fluorescence distribution exhibited no significant difference between BTSL and BTSL-FA. These results indicated that KB cells effectively internalized the FA-conjugated BTSL by FR mediation.

To further confirm the results, the competitive binding of BTSL and BTSL-FA to KB cells or A549 cells was performed by adding excess free folate (1 mM) to block FR binding for 1 h before treatment with liposomes, respectively. The results (Figure 3b) suggested the cellular uptake of BTSL-FA decreased significantly in the presence of free FA in KB cells, becoming almost equivalent to that of BTSL. However, neither the presence or absence of free FA in the culture medium influenced the cellular uptake of BTSL-FA by A549 cells. It was clear that the selectivity of BTSL-FA to KB cells was blocked by free FA.

Based on the preceding cellular uptake experiments, the proposed mechanism of intracellular access enhancement for the BTSL-FA system was as follows: the FA ligand on the BTSL surface was bound to the FR highly expressed tumor cells (KB cells) and enabled the liposomes to achieve the active targeting location to tumor cells; the drug in BTSL-FA rapidly released when subjected to hyperthermia and then diffused into the tumor along a high drug concentration gradient; DOX directly passed through the target cell membrane into cytoplasm and even nuclei to thoroughly destroy the tumor cells.

In addition, the IR780-BTSL-FA drug carrier could enhance DOX delivery into the tumor cell at increased temperature *in vitro* (Figure 4). The absence of a drug group (control) was observed to tolerate temperatures of 42 °C without significant cell damage. In the case of free DOX, the DOX molecule rapidly internalized into cells and bound to nuclei either at 37 or 42 °C, although more drugs were observed in the nuclei when subjected to heating (42 °C).

3.3.2. In Vitro Cytotoxicity. The inhibitory effects on KB cells and A549 cells after incubation with free DOX, IR780-TSL (with or without laser), IR780-BTSL (with or without laser), and IR780-BTSL-FA (with or without laser) were displayed in Figure 5a, respectively. The groups with laser showed higher cell killing potency to both KB cells and A549 cells, which could be interpreted by the increased intracellular concentration of free DOX resulting from photothermally activated temperature-triggered DOX release. On the other hand, IR780-BTSL-FA (with laser) exhibited stronger growth inhibition effect on KB

DOI: 10.1021/acsami.5b06552
ACS Appl. Mater. Interfaces 2015, 7, 20556−20567

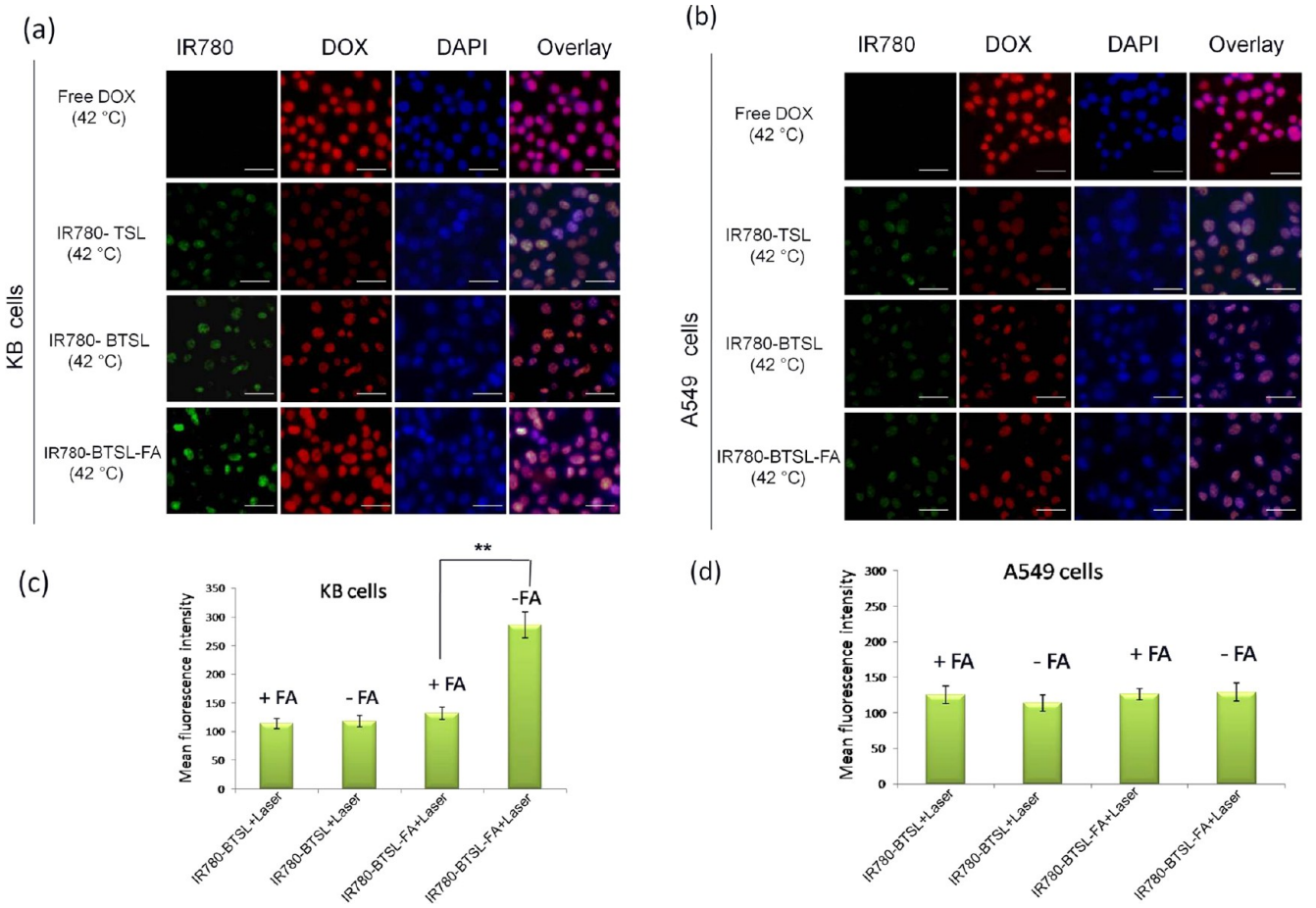

Figure 3. *In vitro* cellular uptake of various formulations into KB cells (a) and A549 cells (b) and with or without free FA (c and d). The scale bar represented 50 μm. The data were presented as the mean ± SD (n = 3). (**) $p < 0.01$.

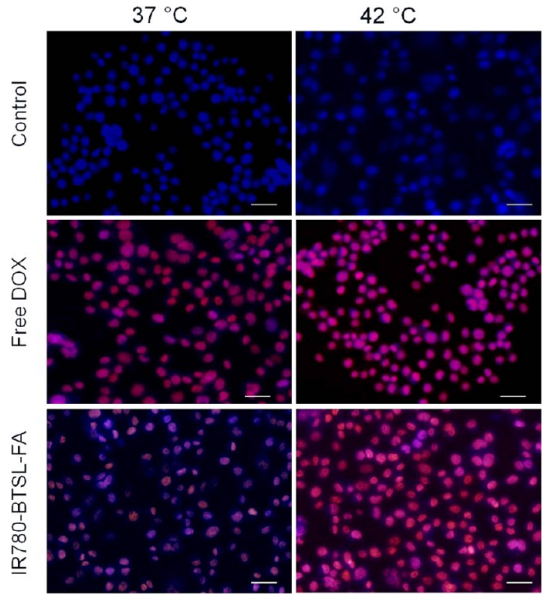

Figure 4. Temperature-induced intracellular drug delivery to KB cells at two different temperatures. The scale bar represented 50 μm.

cells than other formulations, whereas it showed no significant difference with IR780-BTSL (with laser) for A549 cells (IC_{50} values were 46.28 and 48.71 μg/mL, respectively). IR780-BTSL-FA (with laser) showed the strongest cytotoxicity on KB cells, followed by IR780-BTSL (with laser; IC_{50} = 29.83 μg/mL), free DOX (IC_{50} = 28.14 μg/mL), and IR780-TSL (with laser; IC_{50} = 57.89 μ g/mL), respectively. In summary, the *in vitro* cytotoxicity studies indicated that IR780-BTSL-FA combined with laser irradiation promoted antiproliferative activity in KB cells in the presence of overexpressed FR, which was consistent with the cellular uptake studies.

Importantly, IR780-mediated photothermal heating could significantly increase DOX-related toxicity of tumor cells (Figure 5b). Free DOX as well as IR780-BTSL-FA displayed slightly greater cytotoxicity with laser irradiation. The carrier in the absence of DOX (blank IR780-BTSL-FA) exhibited scarcely any cytotoxicity but showed significantly increased cytotoxicity when exposed to laser irradiation. The results indicated that photothermally activated heating by IR780 not only induced drug release from the bubble thermal-sensitive liposomes but also improved cytotoxicity.

3.4. *In Vivo* Targeted Delivery. *3.4.1. In Vivo Imaging and Biodistribution Analysis.* To determine the real-time biodistribution of liposomes, various formulations were injected into tumor-bearing mice via the tail vein. The time-dependent clearance and *in vivo* targeting efficacy of each formulation was observed using noninvasive near-IR imaging in live animals (Figure 6a). The amounts of the IR780-BTSL-FA accumulated in tumor and organs were measured by using the intrinsic near-IR fluorescence of IR780.

After administration of various formulations, mice showed strong fluorescence signals in the liver, suggesting free IR780 and IR780-liposomes were both distributed and metabolized by the

DOI: 10.1021/acsami.5b06552
ACS Appl. Mater. Interfaces 2015, 7, 20556−20567

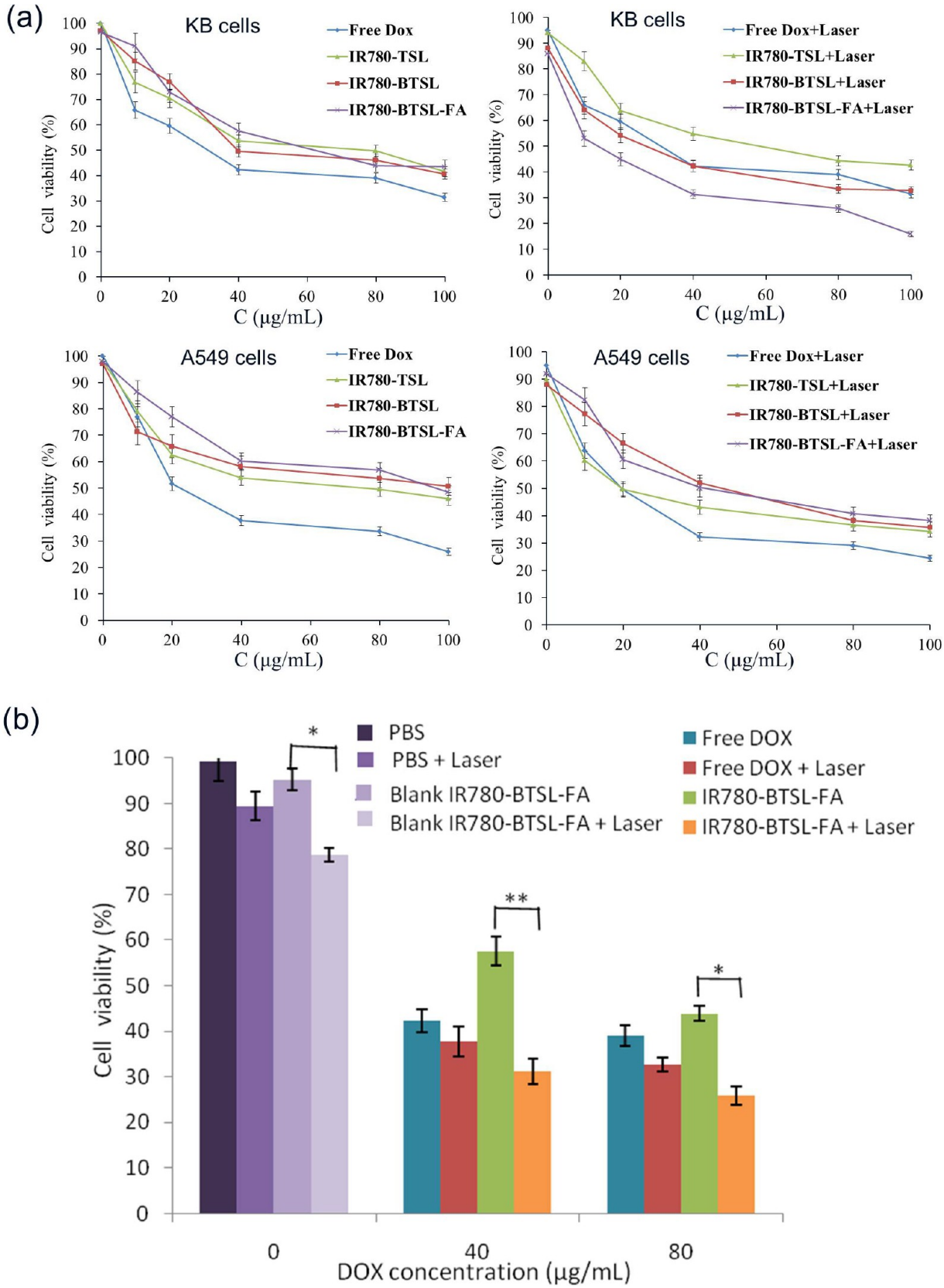

Figure 5. *In vitro* cytotoxicity of (a) various formulations against KB cells and A549 cells following 4 h incubation. (b) Photothermally activated formulations to KB cells with or without near-IR laser irradiation (780 nm, 1 W/cm^2). (*) $p < 0.05$; (**)$p < 0.01$.

liver. However, free IR780 solution showed nonspecific distribution of fluorescence all over the body within 2 h, with rapidly decreased fluorescence signals at 12 h postinjection. On the contrary, the fluorescence was still clearly visible of IR780-TSL, IR780-BTSL, and IR780-BTSL-FA at 12 h after injection, respectively, indicating a prolonged circulation of the PEGylated

DOI: 10.1021/acsami.5b06552
ACS Appl. Mater. Interfaces 2015, 7, 20556−20567

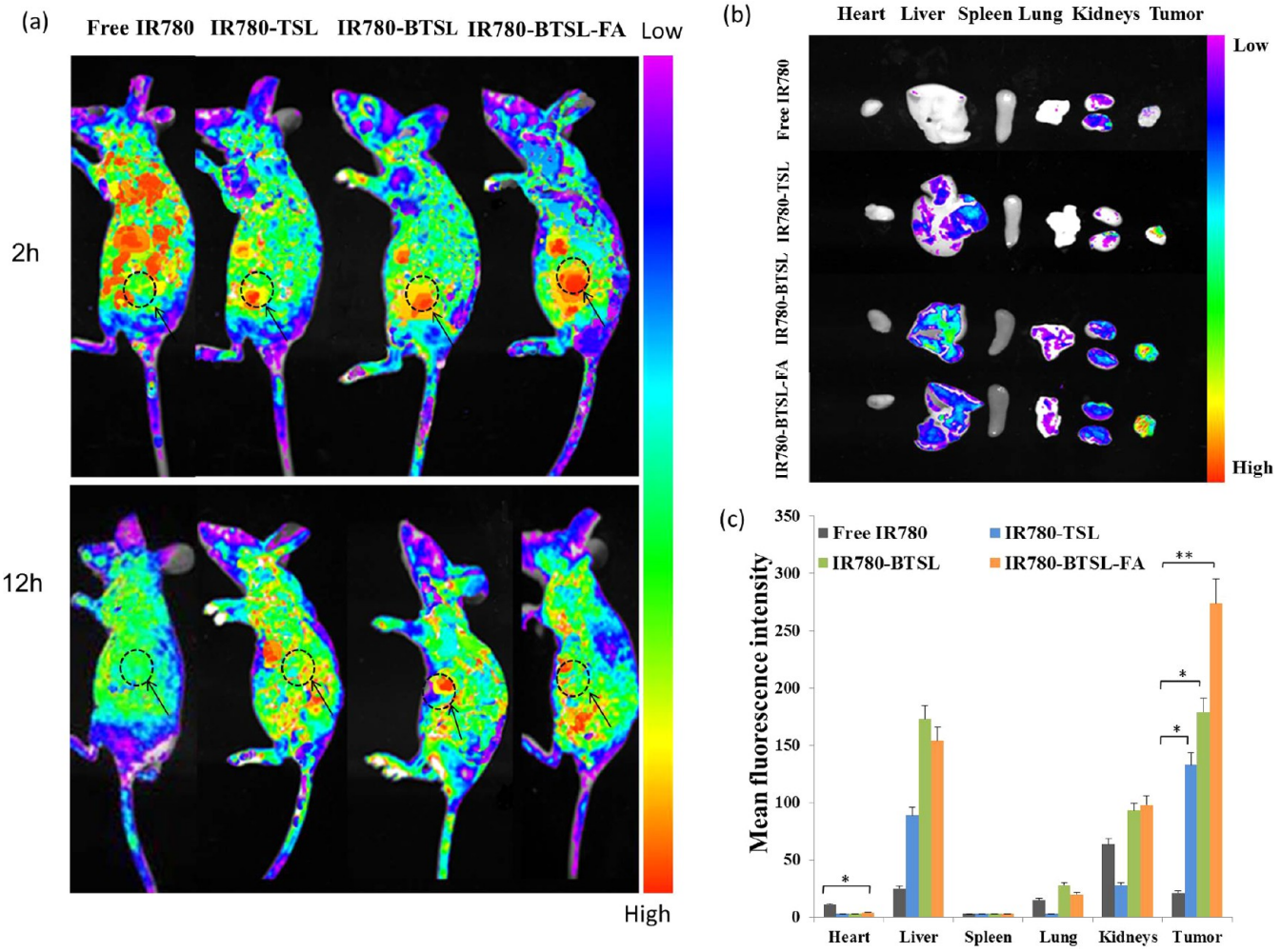

Figure 6. (a) *In vivo* images taken at 2 and 12 h time point. For IR780-TSL, IR780-BTSL, and IR780-BTSL-FA, the nude mice were subjected to near-IR laser irradiation (780 nm, 1 W/cm^2) for 15 min after vein tail injection. (b) Near-IR fluorescence images of major organs and tumors after injection of various formulations at 12 h. (c) Semiquantitative biodistribution in nude mice determined by mean FL intensity of organs and tumor. The data were shown as mean ± SD (n = 6). (*) $p < 0.05$; (**)$p < 0.01$.

nanocarriers. In addition, the BTSL system (BTSL and BTSL-FA) presented significantly improved drug delivery to the tumor site compared to the TSL system, both at 2 and 12 h, suggesting excellent drug release behavior due to the triggered mechanism of the BTSL system. Furthermore, higher drug accumulation in the tumor for IR780-BTSL-FA was observed compared to IR780-BTSL at 2 h. Even at 12 h, IR780-BTSL-FA still retained strong fluorescence intensity around the tumor site, showing the high tumor targeting efficiency of BTSL-FA.

For more accurate measurement, major internal organs (heart, liver, spleen, lung, and kidneys) and tumors were removed at 12 h postinjection and analyzed directly on the near-IR fluorescence imaging system (Figure 6b). As shown in Figure 6b, weak signals were exhibited in the tumors of control mice treated with free IR780. The accumulation of IR780-BTSL-FA in the tumor was much higher than that of IR780-BTSL (1.54 times) and IR780-TSL (2.12 times), indicating its selectively targeted capability in the tumor site. This might have been due to the specific binding between FA ligand and the FA receptor in tumor cells through a receptor-mediated active targeting, demonstrating the advantage of IR780-BTSL-FA for tumor treatment. As reported, DOX was a potent tumor chemotherapeutic agent, but its clinical application was considerably limited by potential lethal cardiotoxicity.[38,39] In this work, it was clear that the BTSL-FA system significantly reduced drug distribution in cardiac tissue compared to free drug (Figure 6b), indicating more excellent therapeutic efficacy and less cytotoxicity of BTSL-FA.

3.4.2. In Vivo Antitumor Efficacy and Toxicity. The antitumor activity of free drug and liposomes in the KB tumor-bearing mice models was studied in this part. As shown in Figure 7c, the tumor volume of the mice subjected to saline as control rapidly increased in 18 days, while the tumor growth for free DOX and liposomal formulations treated groups were significantly suppressed with locally mild hyperthermia. The growth of KB tumors was slightly inhibited by IR780-TSL, IR780-BTSL, and IR780-BTSL-FA without laser irradiation. On the contrary, the laser irradiation group manifested the better antitumor efficacy, indicating that the effect of local photothermal heating could not be negligible.

Notably, IR780-BTSL-FA in combination with laser irradiation demonstrated the greatest inhibitory effect on tumor growth, with significantly decreased tumor volume from 182 to 45 mm^3 (Figure 7b). The results strongly revealed the dual effect of targeting and photothermal therapies for IR780-BTSL-FA. First, under photothermal heating, considerably more DOX were rapid released (as described in *in vitro* release profiles) and

DOI: 10.1021/acsami.5b06552
ACS Appl. Mater. Interfaces 2015, 7, 20556−20567

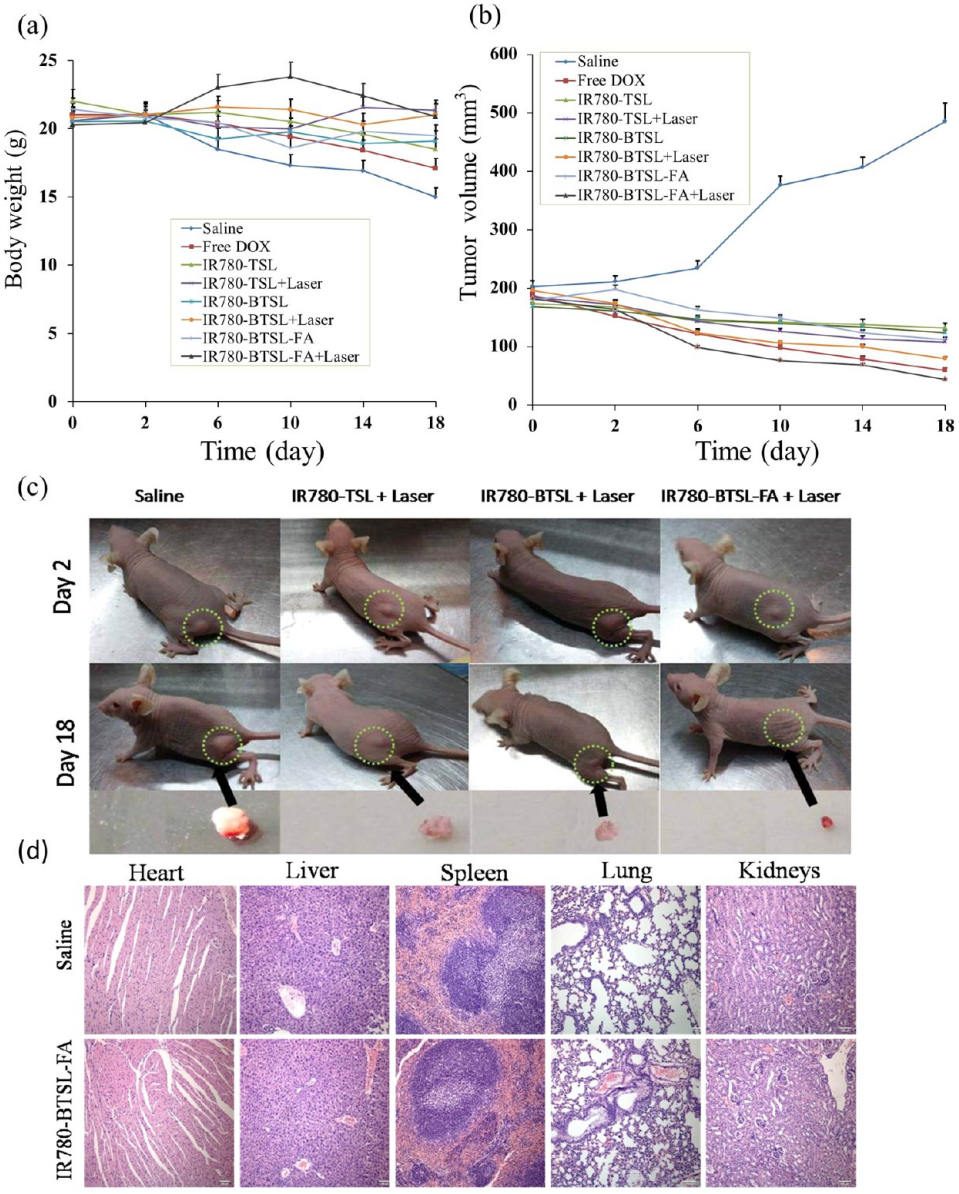

Figure 7. (a) Antitumor activity in nude mice (KB cells implanted) after treatment for 18 days. (b) Body weight changes of the tumor-bearing mice after treatment. (c) Representative photographs of mice bearing KB tumors and excised tumor on 18 days after treatments. The tumor was marked with dashed circles. (d) Histological evaluation of tissues from mice treated with saline and IR780-BTSL-FA (single dose at 10 mg of DOX/kg). Each organ was sliced for hematoxylin and eosin (H&E) staining.

accumulated into tumor cells, resulting in maximum drug exposure in the tumor. Second, active tumor targeting effect caused by FA receptor-mediated endocytosis facilitated higher efficiency than nontargeted liposomes when DOX was delivered to the tumor. What is more, it was reported that the blank BTSL itself was still capable of killing tumor cells since a disruptive force would be produced similar to the cavitation effect induced by ultrasound after the transient formation, growth, and collapse of CO_2 bubbles under mild hyperthermia.[40] The cavitation force acting on lysosomes could mechanically disrupt the membranes to release their proteolytic enzymes into the cytosol, resulting in cell necrosis without leaving behind any toxic agent.[5]

The potential adverse effect of antitumor therapy remained a big problem for future clinical applications. In the present study, the body weight was estimated as an indicator for treatment-induced toxicity. Although the free DOX group showed obviously tumor inhibitory efficiency, it presented a weight loss of more than 25% at 18 days (Figure 7a), indicating the serious toxic side effects. The weight loss of the free DOX group was due to the nontargeted characteristics. Despite the observed weak fluctuations during the treatment period, there was no significant reduction in body weight of the mice groups treated with IR780-BTSL and IR780-BTSL-FA formulations combined with photothermal heating, demonstrating the low toxicity of the BTSL system. This result was further confirmed by organ damage evaluation (Figure 7d). The mice group treated with saline was the control. In summary, as illustrated in the H&E-stained organ tissue slices, no significant necrotic cell was observed in various organs for the IR780-BTSL-FA-treated group, which gave evidence for the excellent safety of IR780-BTSL-FA.

4. CONCLUSIONS

In summary, smart theranostic nanocarrier IR780-BTSL-FA combining the specific targeting effect and hyperthermia-triggered

DOI: 10.1021/acsami.5b06552
ACS Appl. Mater. Interfaces 2015, 7, 20556−20567

drug release characteristics was successfully fabricated in this study. This proposed bubble-generating system IR780-BTSL-FA simultaneously delivering DOX and IR780 to tumor regions showed excellent thermoresponsive properties and strong target effect as well as tumor inhibitory activities compared to free DOX both *in vitro* and *in vivo*. The smart liposomes injected intravenously into tumor-bearing mice could strongly suppress tumor growth under photothermal heating. The *in vivo* biodistribution of IR780-BTSL-FA showed increased accumulation in the irradiated tumor (12.7-fold greater than free solution, 2.1-fold than IR780-TSL). These results clearly proved the theranostic nanocarrier which was capable of enhancing the therapeutic index might be promising as a drug delivery system for imaging-guided tumor therapy.

AUTHOR INFORMATION

Corresponding Authors

* (N.L.) E-mail: linan19850115@163.com.
*(F.P.T.) E-mail: tanfengping@163.com.

Notes

The authors declare no competing financial interest.

ACKNOWLEDGMENTS

This research was supported partially by the National Basic Research Project (Grant 2014CB932200) of the MOST for financial support.

REFERENCES

(1) Fang, J.; Nakamura, H.; Maeda, H. The EPR Effect: Unique Features of Tumor Blood Vessels for Drug Delivery, Factors Involved, and Limitations and Augmentation of the Effect. *Adv. Drug Delivery Rev.* **2011**, *63*, 136−151.

(2) Park, S. M.; Kim, M. S.; Park, S.-J.; Park, E. S.; Choi, K.-S.; Kim, Y.; Kim, H. R. Novel Temperature-Triggered Liposome with High Stability: Formulation, *in Vitro* Evaluation, and *in Vivo* Study Combined with High-Intensity Focused Ultrasound (HIFU). *J. Controlled Release* **2013**, *170*, 373−379.

(3) Seo, H. J.; Kim, J.-C. 7-Acetoxycoumarin Dimer-Incorporated and Folate-Decorated Liposomes: Photoresponsive Release and *in Vitro* Targeting and Efficacy. *Bioconjugate Chem.* **2014**, *25*, 533−542.

(4) Wang, S.; Wang, H.; Liu, Z. Y.; Wang, L. L.; Wang, X. M.; Su, L.; Chang, J. Smart pH- and Reduction-Dual-Responsive Folate−PEG-Coated Polymeric Lipid Vesicles for Tumor-Triggered Targeted Drug Delivery. *Nanoscale* **2014**, *6*, 7635.

(5) Chung, M.-F.; Chen, K.-J.; Liang, H.-F.; Liao, Z.-X.; Chia, W.-T.; Xia, Y.; Sung, H.-W. A Liposomal System Capable of Generating CO2 Bubbles to Induce Transient Cavitation, Lysosomal Rupturing, and Cell Necrosis. *Angew. Chem., Int. Ed.* **2012**, *51*, 10089−10093.

(6) Ashley, C. E.; Carnes, E. C.; Philips, G. K.; Padilla, D.; Durfee, P. N.; Brown, P. A.; Hanna, T. N.; Liu, J.; Phillips, B.; Carter, M. B.; Carroll, N. J.; Jiang, X.; Dunphy, D. R.; Willman, C. L.; Petsev, D. N.; Evans, D. G.; Parikh, A. N.; Chackerian, B.; Wharton, W.; Peabody, D. S.; Brinker, C. J. The Targeted Delivery of Multicomponent Cargos to Cancer Cells by Nanoporous Particle-Supported Lipid Bilayers. *Nat. Mater.* **2011**, *10*, 389−397.

(7) Gao, W.; Xiang, B.; Meng, T. T.; Liu, F.; Qi, X. R. Chemotherapeutic Drug Delivery to Cancer Cells Using a Combination of Folate Targeting and Tumor Microenvironment-Sensitive Polypeptides. *Biomaterials* **2013**, *34*, 4137−4149.

(8) Allen, T. M. Ligand-Targeted Therapeutics in Anticancer Therapy. *Nat. Rev. Cancer* **2002**, *2*, 750−763.

(9) Weitman, S. D.; Lark, R. H.; Coney, L. R.; Fort, D. W.; Frasca, V.; Zurawski, V. R., Jr.; Kamen, B. A. Distribution of the Folate Receptor GP38 in Normal and Malignant Cell Lines and Tissues. *Cancer Res.* **1992**, *52*, 3396−3340.

(10) Ross, J. F.; Chaudhuri, P. K.; Ratnam, M. Differential Regulation of Folate Receptor Isoforms in Normal and Malignant Tissues *in Vivo* and in Established Cell Lines. Physiologic and Clinical Implications. *Cancer* **1994**, *73*, 2432−2443.

(11) Lu, Y.; Low, P. S. Folate-Mediated Delivery of Macromolecular Anticancer Therapeutic Agents. *Adv. Drug Delivery Rev.* **2002**, *54*, 675−693.

(12) Xia, W.; Low, P. S. Folate-Targeted Therapies for Cancer. *J. Med. Chem.* **2010**, *53*, 6811−6824.

(13) Goren, D.; Horowitz, A. T.; Tzemach, D.; Tarshish, M.; Zalipsk, A.; Gabizon, A. Nuclear Delivery of Doxorubicin via Folate-targeted Liposomes with Bypass of Multidrug-resistance Efflux Pump. *Clin. Cancer Res.* **2000**, *6*, 1949−1957.

(14) Sudimack, J.; Lee, R. J. Targeted Drug Delivery via the Folate Receptor. *Adv. Drug Delivery Rev.* **2000**, *41*, 147−162.

(15) Yu, J.; Javier, D.; Yaseen, M. A.; Nitin, N.; Richards-Kortum, R.; Anvari, B.; Wong, M. S. Self-assembly Synthesis, Tumor Cell Targeting, and Photothermal Capabilities of Antibody-Coated Indocyanine Green Nanocapsules. *J. Am. Chem. Soc.* **2010**, *132*, 1929−1938.

(16) Zheng, X.; Xing, D.; Zhou, F.; Wu, B.; Chen, W. R. Indocyanine Green-Containing Nanostructure as Near Infrared Dual-Functional Targeting Probes for Optical Imaging and Photothermal Therapy. *Mol. Pharmaceutics* **2011**, *8*, 447−456.

(17) Zheng, X.; Zhou, F.; Wu, B.; Chen, W. R.; Xing, D. Enhanced Tumor Treatment Using Biofunctional Indocyanine Green-Containing Nanostructure by Intratumoral or Intravenous Injection. *Mol. Pharmaceutics* **2012**, *9*, 514−522.

(18) Yue, C.; Liu, P.; Zheng, M.; Zhao, P.; Wang, Y.; Ma, Y.; Cai, L. IR-780 Dye Loaded Tumor Targeting Theranostic Nanoparticles for NIR Imaging and Photothermal Therapy. *Biomaterials* **2013**, *34*, 6853−6861.

(19) Ju, E.; Li, Z.; Liu, Z.; Ren, J.; Qu, X. Near-Infrared Light-Triggered Drug-Delivery Vehicle for Mitochondria-Targeted Chemo-Photothermal Therapy. *ACS Appl. Mater. Interfaces* **2014**, *6*, 4364−4370.

(20) Soussan, E.; Cassel, S.; Blanzat, M.; Rico-lattes, I. Drug Delivery by Soft Matter: Matrix and Vesicular Carriers. *Angew. Chem., Int. Ed.* **2009**, *48*, 274−288.

(21) Boyer, C.; Zasadzinski, J. A. Multiple Lipid Compartments Slow Vesicle Contents Release in Lipases and Serum. *ACS Nano* **2007**, *1*, 176−182.

(22) Morgan, N. Y.; English, S.; Chen, W.; Chernomordik, V.; Russo, A.; Smith, P. D.; Gandjbakhche, A. Real Time in Vivo Non-invasive Optical Imaging Using Near-Infrared Fluorescent Quantum Dots. *Acad. Radiol.* **2005**, *12*, 313−323.

(23) Yang, Y. F.; Xie, X. Y.; Yang, Y.; Zhang, H.; Mei, X. G. A Review on the Influences of Size and Surface Charge of Liposome on Its Targeted Drug Delivery *in Vivo*. *Acta Pharm. Sin.* **2013**, *48*, 1644−1650.

(24) Torchilin, V. Tumor Delivery of Macromolecular Drugs Based on the EPR Effect. *Adv. Drug Delivery Rev.* **2011**, *63*, 131−135.

(25) Ma, X.; Zhou, J.; Zhang, C. X.; Li, X. Y.; Li, N.; Ju, R. J.; Shi, J. F.; Sun, M. G.; Zhao, W. Y.; Mu, L. M.; Yan, Y.; Lu, W. L. Modulation of Drug-Resistant Membrane and Apoptosis Proteins of Breast Cancer Stem Cells by Targeting Berberine Liposomes. *Biomaterials* **2013**, *34*, 4452−4465.

(26) Al-Jamal, W. T.; Al-Jamal, K. T.; Cakebread, A.; Halket, J. M.; Kostarelos, K. Blood Circulation and Tissue Biodistribution of Lipid−Quantum Dot (L-QD) Hybrid Vesicles Intravenously Administered in Mice. *Bioconjugate Chem.* **2009**, *20*, 1696−1702.

(27) Dicheva, B. M.; ten Hagen, T. L.; Li, L.; Schipper, D.; Seynhaeve, A. L.; van Rhoon, G. C.; Eggermont, A. M.; Lindner, L. H.; Koning, G. A. Cationic Thermosensitive Liposomes: A Novel Dual Targeted Heat-Triggered Drug Delivery Approach for Endothelial and Tumor Cells. *Nano Lett.* **2013**, *13*, 2324−2331.

(28) Al-Ahmady, Z. S.; Al-Jamal, W. T.; Bossche, J. V.; Bui, T. T.; Drake, A. F.; Mason, A. J.; Kostarelos, K. Lipid−Peptide Vesicle Nanoscale Hybrids for Triggered Drug Release by Mild Hyperthermia *In Vitro* and *In Vivo*. *ACS Nano* **2012**, *6*, 9335−9346.

(29) Tian, Q.; Jiang, F.; Zou, R.; Liu, Q.; Chen, Z.; Zhu, M.; Yang, S.; Wang, J.; Wang, J.; Hu, J. Hydrophilic Cu9S5 Nanocrystals: A Photothermal Agent with a 25.7% Heat Conversion Efficiency for

DOI: 10.1021/acsami.5b06552
ACS Appl. Mater. Interfaces 2015, 7, 20556−20567

Photothermal Ablation of Cancer Cells *In Vivo*. *ACS Nano* **2011**, *5*, 9761−9771.
(30) Navarro, F. P.; Berger, M.; Goutayer, M.; Guillermet, S.; Josserand, V.; Rizo, P.; Vinet, F.; Texier, I. A Novel Indocyanine Green Nanoparticle Probe for Non Invasive Fluorescence Imaging*In Vivo*. *Proc. SPIE* **2009**, *7190*, 7190OL.
(31) Zheng, X.; Zhou, F.; Wu, B.; Chen, W. R.; Xing, D. Enhanced Tumor Treatment Using Biofunctional Indocyanine Green-Containing Nanostructure by Intratumoral or Intravenous Injection. *Mol. Pharmaceutics* **2012**, *9*, 514−522.
(32) Chan, J. M.; Zhang, L.; Yuet, K. P.; Liao, G.; Rhee, J.-W.; Langer, R.; Farokhzad, O. C. PLGA−Lecithin−PEG Core−Shell Nanoparticles for Controlled Drug Delivery. *Biomaterials* **2009**, *30*, 1627−1634.
(33) Yue, C.; Liu, P.; Zheng, M.; Zhao, P.; Wang, Y.; Ma, Y.; Cai, L. IR-780 dye loaded Tumor Targeting Theranostic Nanoparticles for NIR Imaging and Photothermal Therapy. *Biomaterials* **2013**, *34*, 6853−6861.
(34) Lim, Y. T.; Noh, Y. W.; Han, J. H.; Cai, Q. Y.; Yoon, K. H.; Chung, B. H. Biocompatible Polymer−Nanoparticle-Based Bimodal Imaging Contrast Agents for the Labeling and Tracking of Dendritic Cells. *Small* **2008**, *4*, 1640−1645.
(35) Tagami, T.; Foltz, W. D.; Ernsting, M. J.; Lee, C. M.; Tannock, I. F.; May, J. P.; Li, S. D. MRI Monitoring of Intratumoral Drug Delivery and Prediction of the Therapeutic Effect with a Multifunctional Thermosensitive Liposome. *Biomaterials* **2011**, *32*, 6570−6578.
(36) Torchilin, V. P. Recent Advances with Liposomes as Pharmaceutical Carriers. *Nat. Rev. Drug Discovery* **2005**, *4*, 145−160.
(37) Tang, Y.; Lei, T.; Manchanda, R.; Nagesetti, A.; Fernandez-Fernandez, A.; Srinivasan, S.; McGoron, A. J. Simultaneous Delivery of Chemotherapeutic and Thermal-Optical Agents to Cancer Cells by a Polymeric (PLGA) Nanocarrier: An *In Vitro* Study. *Pharm. Res.* **2010**, *27*, 2242−2253.
(38) Weiss, R. B. The Anthracyclines: Will We Ever Find a Better Doxorubicin? *Semin. Oncol.* **1992**, *19*, 670−686.
(39) Zhu, Q.; Jia, L. X.; Gao, Z. F.; Wang, C. M.; Jiang, H. Y.; Zhang, J. F.; Dong, L. A Tumor Environment Responsive Doxorubicin-Loaded Nanoparticle for Targeted Cancer Therapy. *Mol. Pharmaceutics* **2014**, *11*, 3269−3278.
(40) Wu, G. H.; Mikhailovsky, A.; Khant, H. A.; Fu, C.; Chiu, W.; Zasadzinski, J. A. Remotely Triggered Liposome Release by Near-Infrared Light Absorption via Hollow Gold Nanoshells. *J. Am. Chem. Soc.* **2008**, *130*, 8175−8177.

DOI: 10.1021/acsami.5b06552
ACS Appl. Mater. Interfaces 2015, 7, 20556−20567